

crystals in gouty tophi.¹ Histological findings did not reveal inflammatory cellular infiltration.

Gouty tophus should be included in the differential diagnosis of the patient considered to have a bone tumor in the hand.

Yukinori Yaegashi, MD

Jun Nishida, MD

Department of Orthopaedic Surgery
Iwate Medical University
Morioka, Japan

Kotaro Oyama, MD

Department of Pediatric Cardiology
Iwate Medical University Memorial Heart Center
Morioka, Japan

<http://dx.doi.org/10.1016/j.jhsa.2012.10.044>

REFERENCE

- Hasselbacher P, Schumacher HR. Immunoglobulin in tophi and on the surface of monosodium urate crystals. *Arthritis Rheum.* 1978;21(3):353–361.

Letter Regarding “Perilunate Dislocations and Fracture Dislocations”

To the Editor:

We read with great interest the article by Jones and Kakar.¹ It nicely covers the whole spectrum of perilunate dislocations and fracture dislocations. The author did not mention the treatment for dislocations in patients who present late. The treatment mentioned is about the salvage procedure directly. It is mentioned in the literature that open reduction internal fixation in a single stage² as well as in a 2-staged procedure³ is a satisfactory procedure if executed properly in patients who present late. The results of these procedures have been satisfactory.⁴ Proximal row carpectomy or wrist arthrodesis might not be acceptable to young patients. Because this injury pattern is mainly seen in young individuals, the option of 2-stage reduction should be given to patients. If this method fails, only then should we proceed to a salvage procedure.

Mohammed Tahir Ansari, MBBS, MS
Department of Emergency Medicine
All India Institute of Medical Sciences
New Delhi, India

Prakash P. Kotwal, MBBS, MS
Department of Orthopaedics
All India Institute of Medical Sciences
New Delhi, India

<http://dx.doi.org/10.1016/j.jhsa.2012.10.047>

REFERENCES

- Jones DB Jr, Kakar S. Perilunate dislocations and fracture dislocations. *J Hand Surg Am.* 2012;37(10):2168–2174.
- Kailu L, Zhou X, Fuguo H. Chronic perilunate dislocations treated with open reduction and internal fixation: results of medium-term follow-up. *Int Orthop.* 2010;34(8):1315–1320.
- Lal H, Jangira V, Kakran R, Mittal D. Two stage procedure for neglected transscaphoid perilunate dislocation. *Indian J Orthop.* 2012;46(3):351–355.

- Garg B, Goyal T, Kotwal PP. Staged reduction of neglected transscaphoid perilunate fracture dislocation: A report of 16 cases. *J Orthop Surg Res.* 2012;7:19.

In Reply:

We thank the reader for the insightful comments and for highlighting several papers^{1–3} (2 of which were published after our manuscript was submitted) addressing the particularly challenging subset of perilunate injuries presenting to the hand surgeon late. Massoud and Naam also recently reported their experience with open reduction internal fixation of perilunate dislocations and fracture dislocations that were treated 13 to 35 weeks from the time of injury, with good to excellent results in 11 of 19 patients.⁴ Although these studies represent relatively small series, they do demonstrate that successful outcomes can be achieved with single-stage or double-stage open reduction internal fixation procedures in the treatment of chronic perilunate injuries. However, the carpus should be easily reducible at the time of surgery, or any form of ligamentous repair can be prone to failure with time. Although these series have not demonstrated loss of intercarpal reduction over time, repair of the intercarpal ligaments can prove challenging secondary to their attenuation and contracture related to the chronicity of the injury. In addition, the articular cartilage must be evaluated at the time of surgery. Kailu et al noted, “With no exception, cases with excellent or good results in this study had satisfactory cartilage condition of the midcarpal joints when evaluated during the operation,” and 2 patients with poor outcomes had been noted to have severe scaphoid and lunate cartilage contusion at the time of open reduction.¹ Therefore, in the setting of severe chondral injury, arthritis, or avascular necrosis associated with a

Colorectal Carcinomas With CpG Island Methylator Phenotype 1 Frequently Contain Mutations in Chromatin Regulators

Tomomitsu Tahara,¹ Eiichiro Yamamoto,^{2,3} Priyanka Madireddi,¹ Hiromu Suzuki,³ Reo Maruyama,³ Woonbok Chung,¹ Judith Garriga,¹ Jaroslav Jelinek,¹ Hiro-o Yamano,⁴ Tamotsu Sugai,⁵ Yutaka Kondo,⁶ Minoru Toyota,^{3,†} Jean-Pierre J. Issa,¹ and Marcos R. H. Estécio^{7,8}

¹Fels Institute for Cancer Research and Molecular Biology, Temple University School of Medicine, Philadelphia, Pennsylvania; ²First Department of Internal Medicine and ³Department of Molecular Biology, Sapporo Medical University, Sapporo, Japan; ⁴Department of Gastroenterology, Akita Red Cross Hospital, Akita, Japan; ⁵Department of Pathology, Iwate Medical University, Morioka, Japan; ⁶Division of Molecular Oncology, Aichi Cancer Center Research Institute, Nagoya, Japan; ⁷Department of Molecular Carcinogenesis and ⁸Center for Cancer Epigenetics, The University of Texas MD Anderson Cancer Center, Houston, Texas

BACKGROUND & AIMS: Subgroups of colorectal carcinomas (CRCs) characterized by DNA methylation anomalies are termed CpG island methylator phenotype (CIMP)1, CIMP2, or CIMP-negative. The pathogenesis of CIMP1 colorectal carcinomas, and their effects on patients' prognoses and responses to treatment, differ from those of other CRCs. We sought to identify genetic somatic alterations associated with CIMP1 CRCs. **METHODS:** We examined genomic DNA samples from 100 primary CRCs, 10 adenomas, and adjacent normal-appearing mucosae from patients undergoing surgery or colonoscopy at 3 tertiary medical centers. We performed exome sequencing of 16 colorectal tumors and their adjacent normal tissues. Extensive comparison with known somatic alterations in CRCs allowed segregation of CIMP1-exclusive alterations. The prevalence of mutations in selected genes was determined from an independent cohort. **RESULTS:** We found that genes that regulate chromatin were mutated in CIMP1 CRCs; the highest rates of mutation were observed in *CHD7* and *CHD8*, which encode members of the chromodomain helicase/adenosine triphosphate–dependent chromatin remodeling family. Somatic mutations in these 2 genes were detected in 5 of 9 CIMP1 CRCs. A prevalence screen showed that nonsilencing mutations in *CHD7* and *CHD8* occurred significantly more frequently in CIMP1 tumors (18 of 42 [43%]) than in CIMP2 (3 of 34 [9%]; $P < .01$) or CIMP-negative tumors (2 of 34 [6%]; $P < .001$). CIMP1 markers had increased binding by CHD7, compared with all genes. Genes altered in patients with CHARGE syndrome (congenital malformations involving the central nervous system, eye, ear, nose, and mediastinal organs) who had *CHD7* mutations were also altered in CRCs with mutations in *CHD7*. **CONCLUSIONS:** Aberrations in chromatin remodeling could contribute to the development of CIMP1 CRCs. A better understanding of the biological determinants of CRCs can be achieved when these tumors are categorized according to their epigenetic status.

most commonly mutations of the *TP53*, *KRAS*, or *APC* gene.^{1,2} In addition, epigenetic alterations in CRCs are also widely reported, mainly gene promoter DNA methylation. Classification of CRCs according to DNA methylation status has identified a subset of tumors with extensive epigenetic instability, characterized by concordant promoter hypermethylation.³ The existence of a CpG island methylator phenotype (CIMP) and its correlation with clinicopathologic features have been confirmed extensively by use of high-throughput techniques.^{4,5} Typical high-level CIMP (CIMP-high, CIMP1) CRCs are associated with microsatellite instability through epigenetic silencing of mismatch repair gene *MLH1*, often have *BRAF* mutation, and occur predominantly in the proximal colon, and low-level CIMP (CIMP-low, CIMP2) has been characterized by DNA methylation of a limited group of genes and mutation of *KRAS*.⁶ Recent pathologic studies have shown that sessile serrated adenomas, mainly observed in the proximal colon, are associated with frequent *BRAF* mutation and CIMP,⁷ suggesting that CIMP-positive CRCs arise from a different precursor than CIMP-negative tumors. Importantly, CIMP-positive CRCs are usually associated with better prognosis,⁸ although patients with CIMP-positive CRC do not benefit from 5-fluorouracil–based adjuvant chemotherapy regimens.⁹

The events that lead to different clinicopathologic manifestations of CIMP1 CRCs are not well described. Although the increased frequency of DNA methylation can determine the behavior of these tumors, it is also possible that somatic mutation of a gene or a group of genes other than *BRAF* that co-occur with CIMP1 modulates the genesis and progression

Keywords: Colon Cancer; Hypermethylation; Microsatellite Instability; Gene Silencing.

[†]Deceased.

Abbreviations used in this paper: CIMP, CpG island methylator phenotype; CRC, colorectal carcinoma; SNP, single-nucleotide polymorphism; TCGA, The Cancer Genome Atlas.

Approximately 75% of all colorectal cancers (CRCs) are sporadic and characterized by genetic lesions,

© 2014 by the AGA Institute
0016-5085/\$36.00

<http://dx.doi.org/10.1053/j.gastro.2013.10.060>

of these tumors. To test this hypothesis, we used next-generation sequencing technology to analyze the exome of 16 colorectal tumors. We found that CIMP1 CRCs have frequent mutations in genes encoding proteins that function in chromatin organization, most frequently *CHD7* and *CHD8*, members of the chromodomain helicase/adenosine triphosphate-dependent (CHD) chromatin remodeling family. These results suggest a prevalent role for aberrant chromatin remodeling in CIMP1 CRCs.

Materials and Methods

Preparation of Clinical Samples

We examined genomic DNA samples from 100 primary CRCs, 10 adenomas, and adjacent normal-appearing mucosae from patients undergoing surgery or colonoscopy at the Johns Hopkins Hospital, Sapporo Medical University, or Akita Red Cross Hospital. Specimens were gathered in accordance with institutional policies and all patients provided written informed consent. All DNA were obtained from frozen specimens, and none of the CRCs had been treated with chemotherapy or radiation. Tumors were selected solely on the basis of availability. Both CRCs and adenomas used in this study were characterized previously for CIMP; microsatellite instability; and *BRAF*, *KRAS*, and *TP53* mutation status.^{6,10} For CIMP classification, DNA methylation of 7 classical markers (*p16*, *MLH1*, *MINT1*, *MINT2*, *MINT12*, *MINT17*, and *MINT31*) was evaluated by bisulfite polymerase chain reaction followed by combined bisulfite restriction analysis (COBRA) or pyrosequencing analysis. Specimens were classified as CIMP1 when *MLH1* and at least 4 of the 6 remaining markers were hypermethylated. CIMP-negative cases presented methylation of none or 1 of the markers, and CIMP2 cases were defined as those with hypermethylation of at least 2 markers but no *MLH1* hypermethylation. Adenomas were classified into CIMP groups according to the methylation profiling of their corresponding carcinoma.

Exome Sequencing

Genomic DNA specimens from 16 colorectal tumors and their adjacent normal tissues were submitted to Otogenetics Corporation (Norcross, GA) for exome capture and sequencing. Briefly, genomic DNA was subjected to agarose gel and optical-density ratio tests to confirm the purity and concentration before fragmentation. Fragmented genomic DNAs were tested for size distribution and concentration using an Agilent Bioanalyzer 2100 (Agilent Technologies, Santa Clara, CA) and a Nanodrop spectrophotometer (Thermo Fisher Scientific, Waltham, MA). Illumina libraries were made from qualified fragmented genomic DNA using Next reagents (New England Biolabs, Ipswich, MA), and the resulting libraries were subjected to exome enrichment using NimbleGen SeqCap EZ Human Exome Library v2.0 (Roche NimbleGen, Inc, Madison, WI) according to manufacturer's instructions. Libraries were tested for enrichment by quantitative polymerase chain reaction and for size distribution and concentration by an Agilent Bioanalyzer 2100. The samples were then sequenced on an Illumina HiSeq2000 (Illumina, Inc, San Diego, CA), which generated paired-end reads of 90 or 100 nucleotides. Reads from both replicates were combined in the final analysis. Data were analyzed for quality, exome coverage, and exome-wide

single-nucleotide polymorphism (SNP)/InDel using the platform provided by DNAnexus (Mountain View, CA).

A sequence variation in tumor DNA was considered a potential somatic mutation when it was present in 3 or more distinct tags of at least 10 total tags. We excluded all variants with a PHRED-encoded probability score <35, those that were present in the DNA of the corresponding normal samples (excluding germline events), and those that were not in coding regions, as well as silent changes and known SNPs (except for clinically associated SNPs). The ratio of variant tag count/reference tag count was also calculated, and all variants with a ratio >0.5 were removed. DNAnexus Genome Browser was used for visual validation of all potential somatic mutations to ensure that they were present in forward and reverse strands.

Pyrosequencing and Sanger Sequencing

Mutations in *CHD7* and *CHD8*, and selected additional mutations in 4 genes detected by exome sequencing (*ITGA10*, *CLSTN2*, *TTN*, and *KCNMA1*), were validated by pyrosequencing or Sanger sequencing. The list of primers is provided in Supplementary Table 4. Pyrosequencing was carried out on a PSQ96 system with a Pyro-Gold reagent Kit (Qiagen, Valencia, CA), and the results were analyzed by PyroMark Q96 ID software version 1.0 (Qiagen). For evaluation of *CHD7* and *CHD8* genes, the coding regions from 94 additional colorectal tumors and matched normal colonic tissues were sequenced using the primers listed in Supplementary Table 11. The sequence chromatograms were visually inspected with DNA Dynamo Sequence Analysis Software (Blue Tractor Software, Llanfairfachan, Wales, UK). All mutations were confirmed by independent sequencing reactions from both forward and reverse strands. Known database polymorphisms were excluded.

Immunohistochemistry Analysis

Expression of *CHD7* (anti-*CHD7* antibody, ab31824; Abcam, Cambridge, MA) and *CHD8* (anti-*CHD8* antibody, ab84527; Abcam) was studied using the DAKO Envision system (DAKO, Carpinteria, CA), as described previously.¹¹

Gene Function Analysis

Functional enrichment of mutated genes was determined by gene ontology analysis using DAVID Bioinformatics Resources 6.7 (<http://david.abcc.ncifcrf.gov/>). *P* values were corrected for multiple hypothesis testing using the Benjamini method. Comparison of the spectrum of mutations in our cohort to known mutations in cancer was done using the Catalogue of Somatic Mutations in Cancer (<http://www.sanger.ac.uk/genetics/CGP/cosmic/>). Gene expression data downloaded from The Cancer Genome Atlas (TCGA) data portal (<https://tcga-data.nci.nih.gov/tcga/>) and published by Lalani et al were subjected to gene set enrichment analysis.¹²

Statistics

The statistical significance of the differential frequency of *CHD7* and *CHD8* mutations in CIMP groups was determined using Fisher's exact test. Two-tailed *P* values were calculated using GraphPad Prism (GraphPad Software, Inc, La Jolla, CA).

Results

Somatic Mutations in 16 Colorectal Tumors Identified by Exome Sequencing

The clinicopathologic data for the 16 cases subjected to exome sequencing are presented in Table 1. These 16 cases consisted of 9 CIMP1 CRCs, 4 CIMP1 adenomas, 1 CIMP2 CRC, and 2 CIMP-negative CRCs. All 9 CIMP1 CRCs presented with microsatellite instability and *MLH1* epigenetic silencing, and 6 of them were known to have mutated *BRAF*. A summary of sequencing statistics for all samples can be found in Supplementary Table 1. On average, approximately 55 million purity-filtered reads were generated for each sample, and 90% of them were aligned to the genome. Samples were sequenced with a 48-fold average exon coverage (ranging from 31- to 68-fold coverage, Supplementary Table 1). Each sample was individually compared with the reference genome (hg19 build 37); single-nucleotide variants, insertions, and deletions were identified by using the DNA Nexus Mapper and nucleotide-level variation tool. Only variations in coding exons were evaluated, and germline variants were identified by comparing the tumor with normal exomes. Known variations reported in the SNP databases were filtered out (except clinically relevant SNPs), and synonymous mutations were excluded. All somatic mutations found in the 16 tumors are presented in detail in Supplementary Table 2 and are summarized in Table 2.

We found a much higher frequency of somatic mutations in CIMP1 CRCs than in other CRCs. On average, there were 425 nonsynonymous mutations per tumor, a 5-fold higher frequency than in tumors previously studied by Sjoblom et al¹³ or Bass et al,¹⁴ which were predominantly microsatellite stable tumors with wild-type *BRAF*. The frequency of mutation in the remaining cases sequenced (4 CIMP1

adenomas, 1 CIMP2 CRC, and 2 CIMP-negative CRCs) was similar to the frequency reported in other CRCs (mean 73 mutations per case) (Supplementary Table 2 and Table 2). Inversely, the nucleotide contexts of the single base substitution mutations were similar among all cases, and C to T and G to A transitions were the most frequent (Supplementary Table 3). To determine the specificity of exome sequencing, 4 randomly selected genes (*TTN*, *ITGA10*, *CLSTN2*, and *KCNMA1*) were resequenced using pyrosequencing and Sanger sequencing (Supplementary Table 4 and Supplementary Figure 1). *BRAF*, *KRAS*, and *TP53* had been previously sequenced in the tumors we used in this study, and their mutation states were included in this analysis. All 24 sequence variants detected by exome sequencing were validated by Sanger or pyrosequencing. Conversely, 12 of 13 (92%) known mutations in these cases were detected by exome sequencing. In terms of frequency of cases with mutations in genes typically associated with colon cancer, we found no mutations in *KRAS* and *SMAD4*, 1 case mutated for each *APC* and *PIK3CA* (6%) and 2 cases mutated for *TP53* (12%). These low frequencies were expected due to the characteristics of our group of samples, which are mostly CIMP1 (81%) or *BRAF* mutated (62%).

Frequent Somatic Mutation of Chromatin Regulators in CIMP1 CRCs

In total, 3169 genes were somatically mutated in at least 1 CIMP1 CRC. Of these, 2615 genes were identified as mutated in other tumor types using the Catalogue of Somatic Mutations in Cancer, and 294 genes were described previously as mutated in tumors from the intestinal tract, including *BRAF*, *APC*, *TP53*, *CTNNB1*, and *PIK3CA*. To filter out genes unrelated to the CIMP phenotype in CRCs, we compared our list of mutated genes in CIMP1 CRCs with the

Table 1. Clinical and Molecular Characteristics of 16 Colorectal Tumors Used in the Discovery Screen

Case	Histology	CIMP status	<i>BRAF</i> mutation ^a	<i>MLH1</i> methylation	MSI status	Age, y	Sex	Source of tumor DNA	Source of matched DNA
C709	Cancer	CIMP1	Wild type	Methylated	MSI	60	F	Primary tumor	Normal colon
C547	Cancer	CIMP1	Wild type	Methylated	MSI	Unknown	F	Primary tumor	Normal colon
C662	Cancer	CIMP1	Wild type	Methylated	MSI	68	F	Primary tumor	Normal colon
C91	Cancer	CIMP1	Mutated	Methylated	MSI	61	M	Primary tumor	Normal colon
C658	Cancer	CIMP1	Mutated	Methylated	MSI	83	M	Primary tumor	Normal colon
C608	Cancer	CIMP1	Mutated	Methylated	MSI	75	F	Primary tumor	Normal colon
C467	Cancer	CIMP1	Mutated	Methylated	MSI	62	M	Primary tumor	Normal colon
C113	Cancer	CIMP1	Mutated	Methylated	MSI	78	M	Primary tumor	Normal colon
C391	Cancer	CIMP1	Mutated	Methylated	MSI	63	M	Primary tumor	Normal colon
Ad1	Adenoma	CIMP1	Mutated	Unmethylated	MSS	75	M	Primary tumor	Normal colon
Ad2	Adenoma	CIMP1	Mutated	Unmethylated	MSS	83	F	Primary tumor	Normal colon
Ad3	Adenoma	CIMP1	Mutated	Unmethylated	MSS	84	F	Primary tumor	Normal colon
Ad4	Adenoma	CIMP1	Mutated	Unmethylated	MSS	77	F	Primary tumor	Normal colon
C108	Cancer	CIMP2	Wild type	Unmethylated	MSS	70	M	Primary tumor	Normal colon
C141	Cancer	CIMP-negative	Wild type	Unmethylated	MSS	60	M	Primary tumor	Normal colon
C126	Cancer	CIMP-negative	Wild type	Methylated	MSI	32	M	Primary tumor	Normal colon

MSI, microsatellite instability; MSS, microsatellite stable.

^aAll samples are *KRAS* wild type. C547, C391, and c141 are *TP53* mutated type; all others are *TP53* wild type.

Table 2. Summary of Mutations in 16 Colorectal Tumors^a

Cases	Total mutations	Nonsynonymous mutations	Stop codon mutations	Insertions	Deletions	SNP	MNP	5'-CpG-3'	5'-TpC-3'	Poly A tract mutations ^b
C709	547	526	21	40	102	392	13	123	36	67
C547	308	294	14	1	17	290	0	174	8	13
C662	94	91	3	0	1	92	1	30	8	2
C91	946	892	54	3	38	886	19	470	25	26
C658	436	411	25	3	15	409	9	175	18	13
C608	525	491	34	13	65	440	7	159	23	55
C467	418	397	21	2	15	394	7	157	21	14
C113	277	264	13	10	49	218	0	66	24	42
C391	278	265	13	0	10	268	0	93	7	9
Ad1	63	61	2	0	0	60	3	22	6	1
Ad2	80	72	8	1	1	74	4	33	5	0
Ad3	82	76	6	0	0	80	2	41	3	0
Ad4	70	65	5	0	1	68	1	32	5	0
C108	24	23	1	1	0	23	0	11	2	1
C141	122	111	11	0	0	118	4	24	4	0
C126	67	61	5	0	1	66	0	21	2	2
Total	4337	4100	236	74	315	3878	70	1631	197	245

SNP, single-nucleotide polymorphisms; MNP, multinucleotide polymorphisms.

^aCIMP1 CRCs: C709, C547, C662, C91, C658, C608, C467, C113, and C391; CIMP1 adenomas: Ad1, Ad2, Ad3 and Ad4; CIMP2 CRC: C108; CIMP-negative CRCs: C141 and C126.

^bPoly A tract was defined as 5 or more repeated sequences of A or T nucleotide.

lists of mutated genes in microsatellite stable, non-*BRAF*-mutated CRCs (likely CIMP-negative cases) reported in 2 exome and whole-genome analyses of colorectal tumors that together evaluated 19 cases (Supplementary Table 5).^{13,14}

As shown in Supplementary Figure 2, the overlap between our list and 1 or both of the other 2 lists was limited to 374 genes, and the majority of mutated genes were exclusive to each group.

We then performed gene ontology analysis to determine whether there was enrichment for specific functional categories among the mutated genes. This analysis showed that mutated genes in CIMP1 CRCs frequently encoded chromatin regulatory proteins ($P = .002$ after Benjamini correction, Supplementary Table 6). Interestingly, this functional category is not represented among the genes exclusively mutated in microsatellite stable or CIMP-negative/wild-type *BRAF* cases or among the genes mutated in both tumor categories. In total, 74 of the mutated genes are included in the chromatin regulation category, and 18 of these were mutated in at least 2 cases (Figure 1 and Supplementary Table 7).

We also evaluated whether mutations in chromatin regulators were enriched in CIMP-positive CRCs in another recent exome study by the TCGA group.¹⁵ We confirmed that enrichment of mutation in these 74 genes was seen more often in CIMP-high CRCs in the TCGA dataset than in CIMP-low and CIMP-negative cases (Figure 1). Among the mutated chromatin regulatory genes, lysine (K)-specific demethylase and CHD groups were particularly notable, with 6 and 5 mutated cases, respectively, in the 9 CIMP1 CRCs. Myeloid/lymphoid or mixed-lineage leukemia and SWI/SNF-related, matrix-associated, actin-dependent regulator of chromatin subfamily groups were also frequently

mutated in CIMP1 CRCs (4 cases for both groups). Although the rate of mutations in chromatin-related genes in CIMP1 adenoma cases was much lower, still 3 of 4 CIMP1 adenomas analyzed had at least 1 mutation in a chromatin-related gene.

CHD7 and CHD8 Are Frequently Mutated in CIMP1 CRCs

Among the recurrently mutated chromatin regulatory genes, the most frequently mutated was *CHD7* (mutated in 4 cases), which encodes a member of the CHD gene family. Another member of this protein family, *CHD8*, is also present in the shortlist of candidate genes and was mutated in 3 cases. Together these 2 genes account for mutations in >50% of the evaluated CIMP-positive CRCs (5 of 9 cases).

Because we compared the mutation results obtained in CIMP1 tumors with those previously published in putatively non-CIMP1 tumors, we performed a prevalence study to rule out any bias in the discovery part of this study. To confirm the association of *CHD7* and *CHD8* mutations with CIMP1, we performed Sanger sequencing of these genes in 94 additional colorectal tumors and matched normal tissues (88 CRCs and 6 adenomas: 29 were CIMP1-, 33 CIMP2-, and 32 CIMP-negative; Supplementary Table 8). The 2 cohorts encompassed 110 colon tumors, including 42 CIMP1-, 34 CIMP2-, and 34 CIMP-negative cases. Representative sequencing chromatograms are presented in Supplementary Figure 3. We found 23 cases with *CHD7* or *CHD8* nonsilent mutations. One tumor had 3 mutations, 4 had 2 mutations, and 18 had a single mutation, for a total of 29 mutations in these genes (Supplementary Table 9). Of these 29 *CHD7* and *CHD8* mutations, 24 could be compared with matched

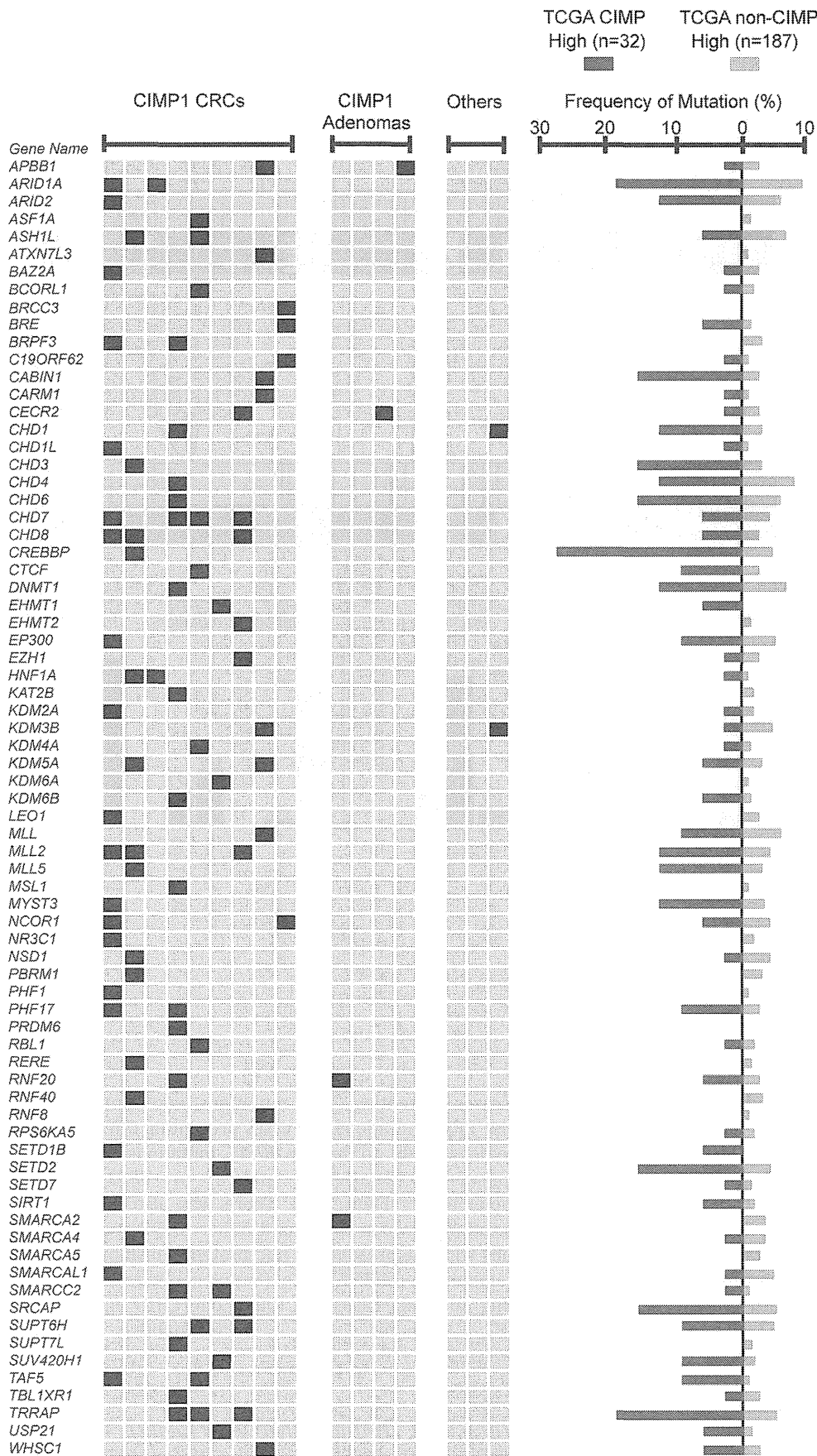


Figure 1. The landscape of mutations in chromatin regulator genes identified by exome sequencing. Each row is a gene and each column is a different case. Each of the 74 chromatin regulator genes in which a mutation has been identified is listed on the left (black, mutated; light gray, wild type). The prevalence of mutations in these 74 genes in the TCGA data is shown at the right (dark gray, CIMP-high cases; light gray, non-CIMP-high cases).

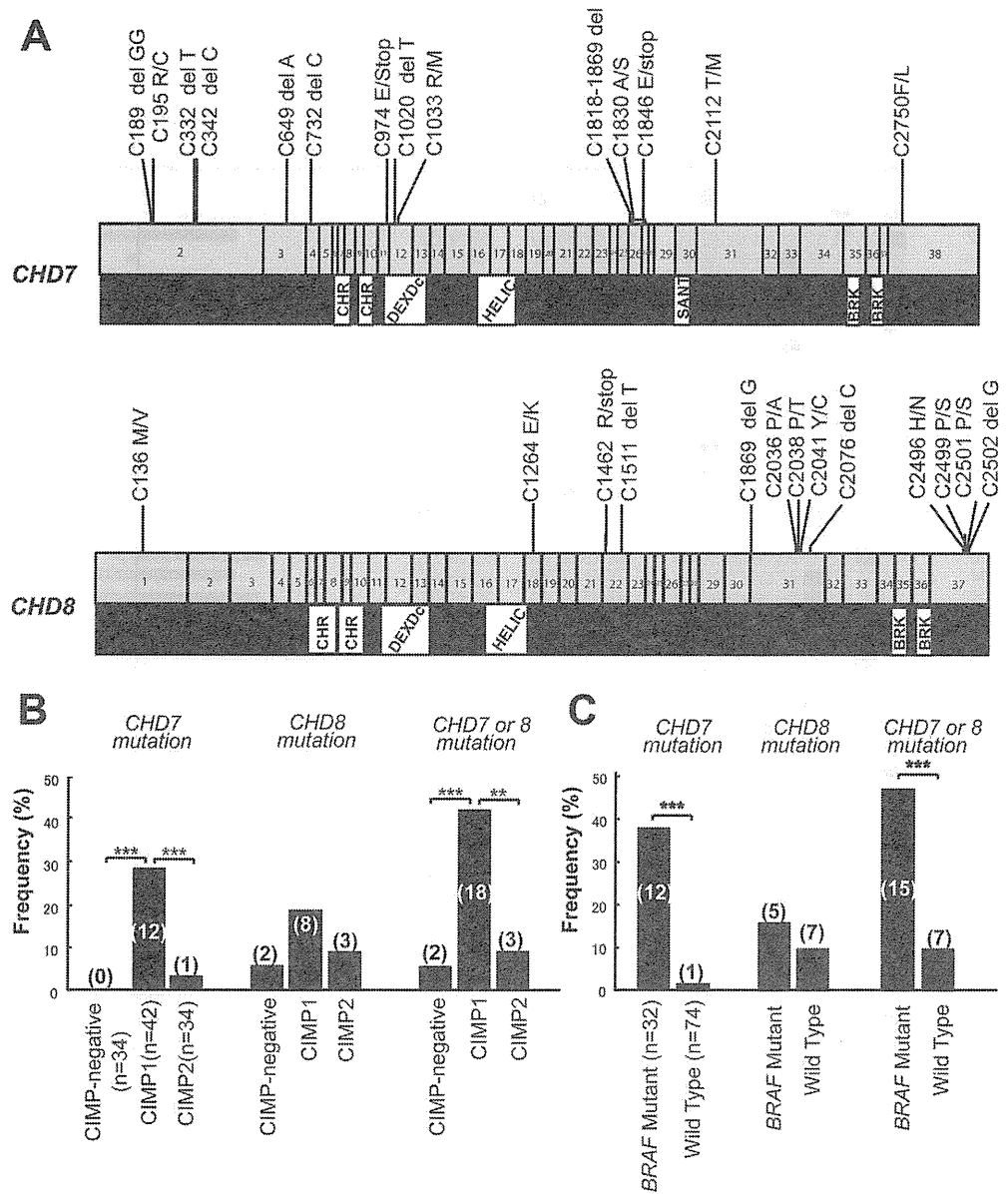


Figure 2. (A) Mutation spectrum of *CHD7* and *CHD8* in 110 colon tumors. Individual exons are represented as numbered boxes. Complementary DNA and peptide positions are based on the transcript IDs NM_017780 (*CHD7*) and NM_001170629 (*CHD8*). CHR, chromatin organization modifier domain; DEXDc, DEAD-like helicase superfamily; HELIC, helicase superfamily C-terminal domain; SANT, "SWI3, ADA2, N-CoR, and TFIIB" DNA-binding domains; BRK, BRK domain. (B, C) Prevalence of *CHD7* and *CHD8* mutations by (B) CIMP status or (C) *BRAF* mutation status. Numbers in parentheses represent numbers of mutated cases. ** $P < .01$, *** $P < .001$.

normal tissues, and the remaining 5 had no matched normal tissue DNA and were compared with a reference human sequence database. The 29 nonsilent *CHD7/CHD8* mutations were distributed throughout the coding region, and 20 of them (69%) were predicted to either truncate the protein through base substitutions, resulting in a stop codon (3 mutations) or a frame deletion (12 mutations), or to damage the protein as predicted by SIFT (sorting intolerant from tolerant) analysis (5 mutations). With the exception of 2 cases with biallelic mutation of *CHD7*, all remaining variations were monoallelic. We found a significant difference in the somatic mutation rate of *CHD7* and *CHD8* genes across the molecular subtypes of colorectal tumors, with a higher incidence of mutations in the CIMP1 tumors (18 of 42 [42.9%]) than in the CIMP2 (3 of 34 [8.8%]; $P < .01$) or CIMP-negative tumors (2 of 34 [5.9%]; $P < .001$; Figure 2B).

The cases presenting *CHD7* mutations were more likely to harbor *BRAF* mutations and cases presenting *CHD7* or *CHD8* were less likely to harbor *KRAS* mutations (Figure 2C, Supplementary Figure 4A and C) or *TP53* mutation (Supplementary Figure 4B). There was also a significant association between *CHD7* and either *CHD7* or *CHD8* mutations with the presence of microsatellite instability, which is common in CIMP1 CRCs (Supplementary Figure 4D). Among adenoma cases, we found one *CHD7* mutant in a CIMP1 adenoma with microsatellite instability (Supplementary Table 9).

Genes That Define CIMP Are CHD7 Targets

The consequences of *CHD7* or *CHD8* mutation are not well established. To get insight into the functions of these

genes, we mined diverse databases. *CHD7* is the most studied of the 2 genes, and mutations in *CHD7* have been reported as causative alterations in CHARGE syndrome, a complex of multiple congenital malformations involving the central nervous system, eye, ear, nose, and mediastinal organs.¹⁶ We first compared distribution of *CHD7* mutations in CHARGE syndrome and CRC. From a total of 703 mutations in the *CHD7* database (www.chd7.org), we focused on 429 nonsilent pathogenic coding sequence mutations (Supplementary Figure 5, Supplementary Table 10). The most prevalent types in both CHARGE syndrome (52%) and CRC (50%) were frameshift deletions or insertions, and nonsense mutations were more frequent in CHARGE (36%) than in CRC (14%). By contrast, missense mutations were more frequent in CRC (36%) than in CHARGE (12%) (Supplementary Figure 5B). The mutations were distributed along the entire coding region, being most frequent in exon 2 in both groups, probably because it has the largest genomic size (Supplementary Figure 5A, Supplementary Table 10). Approximately 21% of the mutations were found in the regions of *CHD7* that encode for the functional domains, and all variations in CRCs observed in functional domains were located in the DEAD-like helicase superfamily (DEXDc) domain. Because the encoded region of these domains is approximately 23% of *CHD7*, the frequency of mutations within these domains is almost the same as those outside if the mutations were distributed equally (Supplementary Figure 5C).

To further assess the relationship between *CHD7* and CIMP, we analyzed publicly available data to see whether altered genes in CIMP-positive CRCs are regulated by *CHD7*.¹⁷⁻¹⁹ We found that frequently methylated genes in CIMP-positive CRCs had significantly higher enrichment of *CHD7* occupancy in their mouse homologue genes in neural stem cells ($P = .003$ compared with all genes; Supplementary Figure 6A) and were enriched among genes that responded to *CHD7* gene knockdown in mouse embryonic stem cells ($P < .00001$ compared with all genes; Supplementary Figure 6B). Finally, we asked whether genes dysregulated in the CHARGE syndrome are also dysregulated in *CHD7*-mutant CRCs. For this, we downloaded level 3 gene expression data from the CRC series studied by the TCGA group.¹⁵ Using gene set enrichment analysis, we asked whether genes up-regulated and down-regulated in CHARGE syndrome¹² are enriched among genes that distinguish *CHD7*-mutant from wild-type CRCs. We found that genes up-regulated in CHARGE syndrome are enriched among genes up-regulated in *CHD7*-mutant CRCs (false discovery rate = 0.04) and, in contrast, genes down-regulated in CHARGE syndrome are enriched among genes that are down-regulated in *CHD7*-mutant CRCs (false discovery rate = 0.07; Supplementary Figure 7). Taken together, these results indicate that the mutations in *CHD7* observed in CRCs are in many aspects functionally similar to those present in CHARGE syndrome, with effects in the regulation of dozens of genes.

Finally, we attempted to link *CHD7/8* mutations to protein levels in cancer. We identified a group of 13 samples used in the discovery and validation steps for which

paraffin-embedded tissues were available and immunohistochemistry was done for the tumors and their normal counterparts. Eleven of these were CIMP1 according to our definition, and the 2 remaining samples were CIMP-negative. Nuclear expression of these proteins was found in normal colon for all cases, and both *CHD7* and *CHD8* were variably expressed in cancers independent of their mutation status (Supplementary Figure 8). The monoallelic and single amino acid change state of the mutations can explain why changes in protein levels were not detected.

Discussion

We found that CIMP1 CRCs have frequent mutations in genes encoding proteins that function in chromatin modification, most frequently *CHD7* and *CHD8*, members of the lysine-specific demethylases and chromodomain helicase/adenosine triphosphate-dependent chromatin remodeling family. Molecular targets of CIMP were enriched among *CHD7*-regulated genes, and genes altered in the CHARGE syndrome with *CHD7* mutations were also altered in *CHD7*-mutant CRCs. Our data are consistent with a function of these proteins in the pathology of CIMP1 CRCs.

A confounding factor in any study that arranges tumors into CIMP groups is the criteria used for classification, as diverse strategies have been proposed and use as few as 5 to as many as 100 markers for this. Here we adopted the criterion first introduced by Toyota et al³ and further refined by Shen et al,⁶ in which 3 groups are defined based on selected markers that include hypermethylation of *MLH1* as a distinctive feature: CIMP1, CIMP2, and CIMP-negative. These groups are mostly equivalent to CIMP-high, CIMP-low, and CIMP-negative groups later defined by high throughput methylation analysis.^{15,18} In our sequencing studies, CIMP1 CRCs presented a higher frequency of somatic mutations than CIMP1 adenomas, CIMP2 CRCs, or CIMP-negative CRCs. It is possible that the higher mutation rate in CIMP1 CRCs is linked to their mismatch repair deficiency. CIMP1 CRCs presented increased mutation in polynucleotide tracts. However, most exome mutations in CIMP1 CRCs were outside polynucleotide tracts, and one CIMP-negative, microsatellite unstable cancer we sequenced had relatively few mutations (Table 2). It is also possible that the higher mutation rate in CIMP1 CRCs is due to other factors: for example, the DNA repair gene *MGMT* was methylated in 5 of the 9 CIMP1 CRCs and in none of the other cases. The hypermutable tendency of CIMP high tumors has been described recently.¹⁵

Genes coding chromatin-related function have been reported previously as a frequent target in other tumor types,²⁰⁻²² but have never been clearly associated with specific subsets (eg, CIMP1 CRC). This highlights the importance of considering both genetics and epigenetics in classifying tumors for improving our understanding of the genesis and therapy for each individual tumor. Because CIMP1 CRCs differ from other CRCs in their pathologic origin, prognosis, and response to treatment,⁷⁻⁹ the data suggest that the distinct genetic background reflects unique characteristics of CIMP1 cases. Unlike gliomas, the tumors

examined here had mutations in neither *IDH1* nor members of its family, indicating that different tumor types have different genetic/epigenetic interactions. Our prevalence study in a series of 94 colorectal tumors confirmed that *CHD7/CHD8* mutations occurred more frequently in CIMP1 tumors than in other CIMP groups. *CHD7* is widely expressed in many tissue types¹⁶ and plays many roles in cellular differentiation^{19,23} and chromatin regulation, including a putative role in protecting chromatin from polycomb-mediated repression.²⁴ Participation of *CHD8* in chromatin insulation has been proposed on the basis of its interaction with the well-characterized insulator protein CTCF.^{25,26} On the basis of their function, we propose that mutations of *CHD7* and *CHD8* in CRCs result in an altered pattern of chromatin modifications and structure, which causes dysregulation of expression of dozens to hundreds of genes.

There is evidence that *CHD* genes participate in cancer. For example, *PVT1-CHD7* gene fusions have been identified in small-cell lung cancer cell lines, and a subset of gastric and colorectal cancers with microsatellite instability presented *CHD7/8* frameshift mutations in mononucleotide repeats that were associated with lower expression of *CHD8* protein.^{27,28} In addition, mutations in *CHD5* were recently discovered in human breast cancer and neuroblastoma,²⁹ and the function of this gene as a tumor suppressor has been confirmed.³⁰ The 29 nonsilent mutations of *CHD7/8* that we identified were distributed throughout the coding region, and 69% of them (20 of 29) were predicted to truncate or damage the protein with no hot spots, a pattern concordant with that observed in tumor suppressor genes.

We also found compelling evidence that there is an overlap between genes targeted or regulated by *CHD7* and CIMP markers. Frequently methylated genes in CIMP-positive CRCs have significantly higher enrichment of *CHD7* occupancy in mouse neural stem cells and among genes regulated by *CHD7* in mouse embryonic stem cells. Evidence of a role for *CHD7* in cancer is also still lacking. In animal models, mice with homozygous *CHD7* mutations die in utero, and heterozygous mice have reduced survival at weaning.¹⁶ No long-term studies could have been conducted in these models. In both CHARGE syndrome and CRC, approximately 80% of *CHD7* mutations are located outside of functional domains, suggesting that even mutations outside of key domains interfere with the gene function. Our findings and the report that a member of the CHD gene family has been proved to be a tumor suppressor gene³⁰ warrant evaluation of *CHD7* and *CHD8* function in colorectal tumorigenesis.

When comparing CIMP1 CRCs and adenomas, the rate of mutations in chromatin-related genes was much lower in CIMP1 adenomas. Still, 3 of the 4 CIMP1 adenomas analyzed had at least 1 mutation in a chromatin-related gene, and 1 CIMP1 adenoma in the prevalence screen presented a mutation in *CHD7* (Figure 1 and Supplementary Tables 7 and 9). In addition, the fact that *CHD7* and *CHD8* mutations were observed in subsets of microsatellite stable CRCs in our study and another study¹⁵ indicates that they are not simply a consequence of defective mismatch repair. Additional functional analyses are required to better assess the

function of mutations in chromatin remodeling genes in the colorectal tumorigenesis process.

The inverse relationship between the *CHD7/8* mutations and the *TP53* inactivating mutation suggests that *CHD7/8* and *TP53* mutations drive different subsets of CRCs. Mutation of genes encoding chromatin-remodeling enzymes can result in an alternative pathway of carcinogenesis independent of *TP53* that drives cancer progression through epigenetic disturbance. The discovery of frequent chromatin regulator mutations in CIMP1 CRCs emphasizes the importance of a better understanding of pathway-specific molecular changes in subsets for targeted therapy and raises the possibility that specific epigenetic therapy targeting alterations in chromatin-remodeling proteins can be useful in treating CIMP1 CRCs.

Supplementary Material

Note: To access the supplementary material accompanying this article, visit the online version of *Gastroenterology* at www.gastrojournal.org, and at <http://dx.doi.org/10.1053/j.gastro.2013.10.060>.

References

1. Rustgi AK. The genetics of hereditary colon cancer. *Genes Dev* 2007;21:2525–2538.
2. Walther A, Johnstone E, Swanton C, et al. Genetic prognostic and predictive markers in colorectal cancer. *Nat Rev Cancer* 2009;9:489–499.
3. Toyota M, Ohe-Toyota M, Ahuja N, et al. Distinct genetic profiles in colorectal tumors with or without the CpG island methylator phenotype. *Proc Natl Acad Sci U S A* 2000;97:710–715.
4. Estecio MR, Yan PS, Ibrahim AE, et al. High-throughput methylation profiling by MCA coupled to CpG island microarray. *Genome Res* 2007;17:1529–1536.
5. Weisenberger DJ, Siegmund KD, Campan M, et al. CpG island methylator phenotype underlies sporadic microsatellite instability and is tightly associated with BRAF mutation in colorectal cancer. *Nat Genet* 2006;38:787–793.
6. Shen L, Toyota M, Kondo Y, et al. Integrated genetic and epigenetic analysis identifies three different subclasses of colon cancer. *Proc Natl Acad Sci U S A* 2007;104:18654–18659.
7. Leggett B, Whitehall V. Role of the serrated pathway in colorectal cancer pathogenesis. *Gastroenterology* 2010;138:2088–2100.
8. Ogino S, Nosho K, Kirkner GJ, et al. CpG island methylator phenotype, microsatellite instability, BRAF mutation and clinical outcome in colon cancer. *Gut* 2009;58:90–96.
9. Jover R, Nguyen TP, Perez-Carbonell L, et al. 5-Fluorouracil adjuvant chemotherapy does not increase survival in patients with CpG island methylator phenotype colorectal cancer. *Gastroenterology* 2011;140:1174–1181.
10. Kimura T, Yamamoto E, Yamano HO, et al. A novel pit pattern identifies the precursor of colorectal cancer derived from sessile serrated adenoma. *Am J Gastroenterol* 2012;107:460–469.

11. Sugai T, Habano W, Uesugi N, et al. Three independent genetic profiles based on mucin expression in early differentiated-type gastric cancers—a new concept of genetic carcinogenesis of early differentiated-type adenocarcinomas. *Mod Pathol* 2004;17:1223–1234.
12. Lalani SR, Safiullah AM, Fernbach SD, et al. Spectrum of CHD7 mutations in 110 individuals with CHARGE syndrome and genotype-phenotype correlation. *Am J Hum Genet* 2006;78:303–314.
13. **Sjobern T, Jones S, Wood LD, Parsons DW**, et al. The consensus coding sequences of human breast and colorectal cancers. *Science* 2006;314:268–274.
14. **Bass AJ, Lawrence MS**, Brace LE, et al. Genomic sequencing of colorectal adenocarcinomas identifies a recurrent VTI1A-TCF7L2 fusion. *Nat Genet* 2011;43:964–968.
15. The Cancer Genome Atlas Research Network. Comprehensive molecular characterization of human colon and rectal cancer. *Nature* 2012;487:330–337.
16. **Janssen N, Bergman JE**, Swertz MA, et al. Mutation update on the CHD7 gene involved in CHARGE syndrome. *Hum Mutat* 2012;33:1149–1160.
17. **Engelen E, Akinci U**, Bryne JC, et al. Sox2 cooperates with Chd7 to regulate genes that are mutated in human syndromes. *Nat Genet* 2011;43:607–611.
18. Hinoue T, Weisenberger DJ, Lange CP, et al. Genome-scale analysis of aberrant DNA methylation in colorectal cancer. *Genome Res* 2012;22:271–282.
19. **Schnetz MP, Handoko L**, Akhtar-Zaidi B, et al. CHD7 targets active gene enhancer elements to modulate ES cell-specific gene expression. *PLoS Genet* 2010;6:e1001023.
20. Jones S, Wang TL, Shih le M, et al. Frequent mutations of chromatin remodeling gene ARID1A in ovarian clear cell carcinoma. *Science* 2010;330:228–231.
21. **van Haaften G, Dalglish GL, Davies H**, et al. Somatic mutations of the histone H3K27 demethylase gene UTX in human cancer. *Nat Genet* 2009;41:521–523.
22. Wilson BG, Roberts CW. SWI/SNF nucleosome remodelers and cancer. *Nat Rev Cancer* 2011;11:481–492.
23. Bajpai R, Chen DA, Rada-Iglesias A, et al. CHD7 cooperates with PBAF to control multipotent neural crest formation. *Nature* 2010;463:958–962.
24. Srinivasan S, Dorigi KM, Tamkun JW. Drosophila Kismet regulates histone H3 lysine 27 methylation and early elongation by RNA polymerase II. *PLoS Genet* 2008;4:e1000217.
25. Huang S, Li X, Yusufzai TM, et al. USF1 recruits histone modification complexes and is critical for maintenance of a chromatin barrier. *Mol Cell Biol* 2007;27:7991–8002.
26. Ishihara K, Oshimura M, Nakao M. CTCF-dependent chromatin insulator is linked to epigenetic remodeling. *Mol Cell* 2006;23:733–742.
27. Kim MS, Chung NG, Kang MR, et al. Genetic and expression alterations of CHD genes in gastric and colorectal cancers. *Histopathology* 2011;58:660–668.
28. Pleasance ED, Stephens PJ, O'Meara S, et al. A small-cell lung cancer genome with complex signatures of tobacco exposure. *Nature* 2010;463:184–190.
29. Bagchi A, Mills AA. The quest for the 1p36 tumor suppressor. *Cancer Res* 2008;68:2551–2556.
30. Bagchi A, Papazoglu C, Wu Y, et al. CHD5 is a tumor suppressor at human 1p36. *Cell* 2007;128:459–475.

Author names in bold designate shared co-first authorship.

Reprint requests

Address requests for reprints to: Marcos R. H. Estécio, PhD, Department of Molecular Carcinogenesis, The University of Texas MD Anderson Cancer Center, 1515 Holcombe Boulevard, Houston, Texas 77030. e-mail: mestecio@mdanderson.org; fax: (512) 237-3439.

Acknowledgments

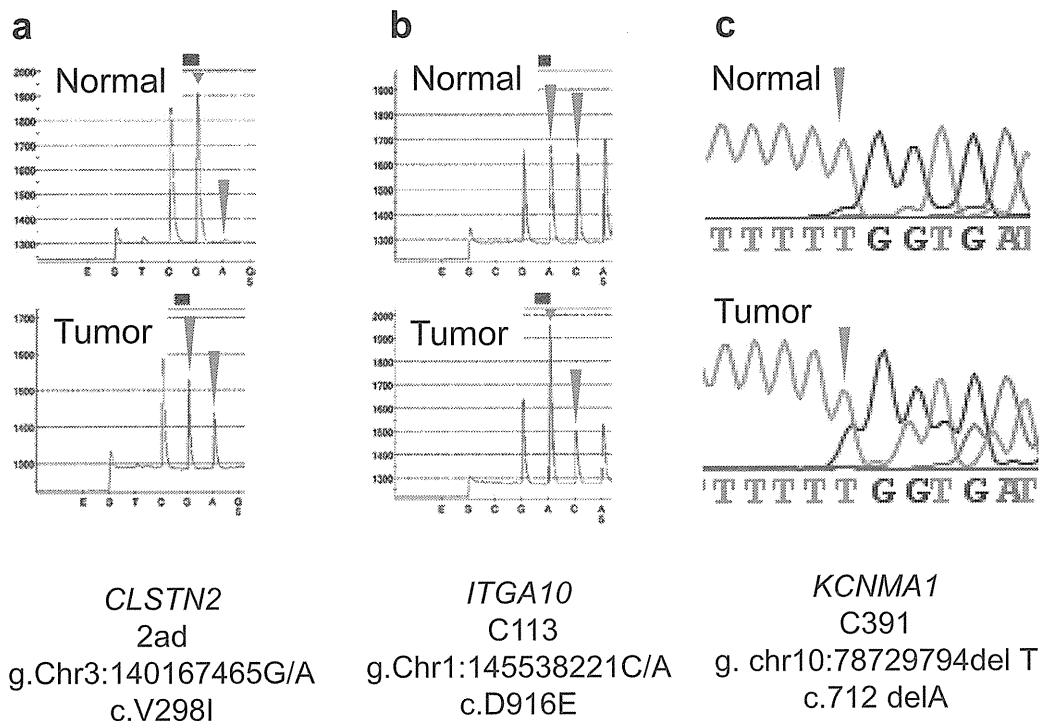
The authors thank Kathryn L. Hale for proofreading the manuscript.

Conflicts of interest

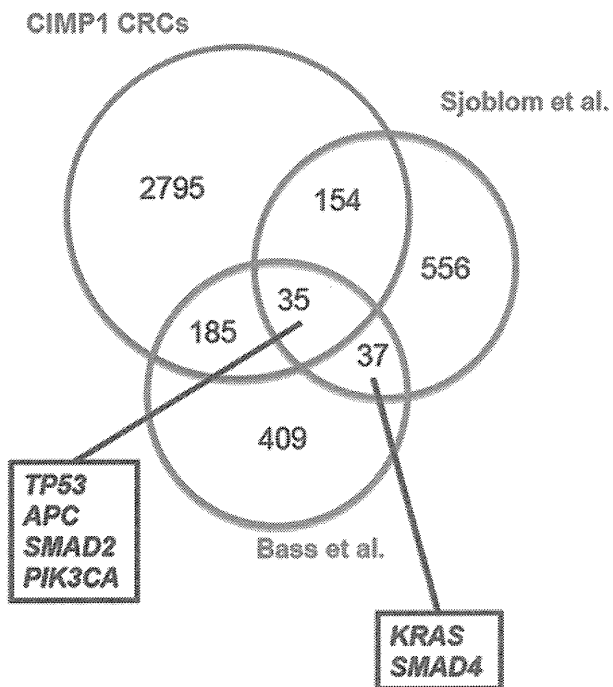
The authors disclose no conflicts.

Funding

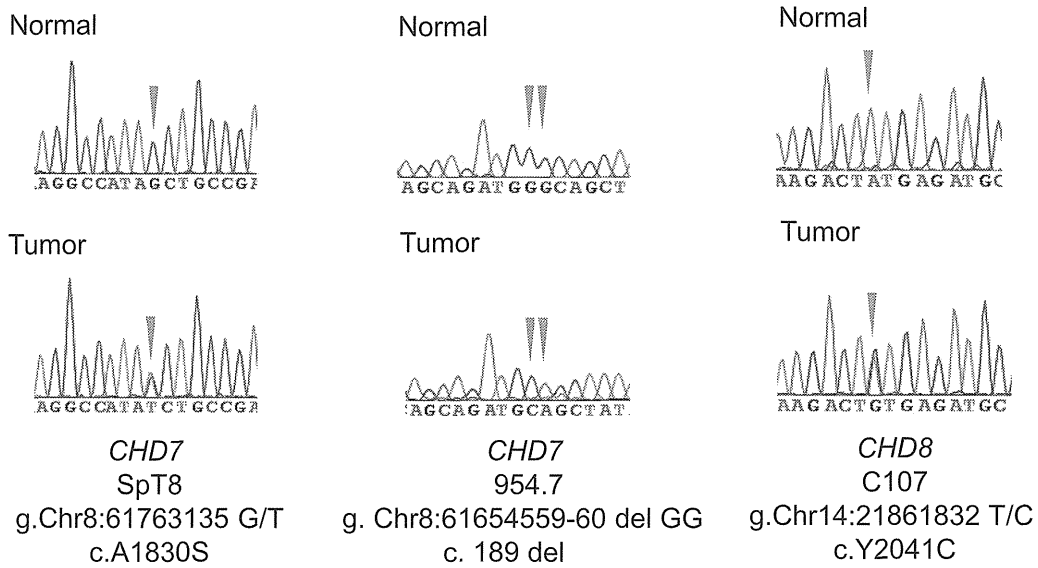
This work was supported by the G.S. Hogan Gastrointestinal Research Fund of The University of Texas MD Anderson Cancer Center (to M.R.H.E.) and by National Institutes of Health grants CA158112, CA098006, and CA100632 to J.-P.J.I. J.-P.J.I. is an American Cancer Society Clinical Research professor supported by a generous gift from the F.M. Kirby Foundation.



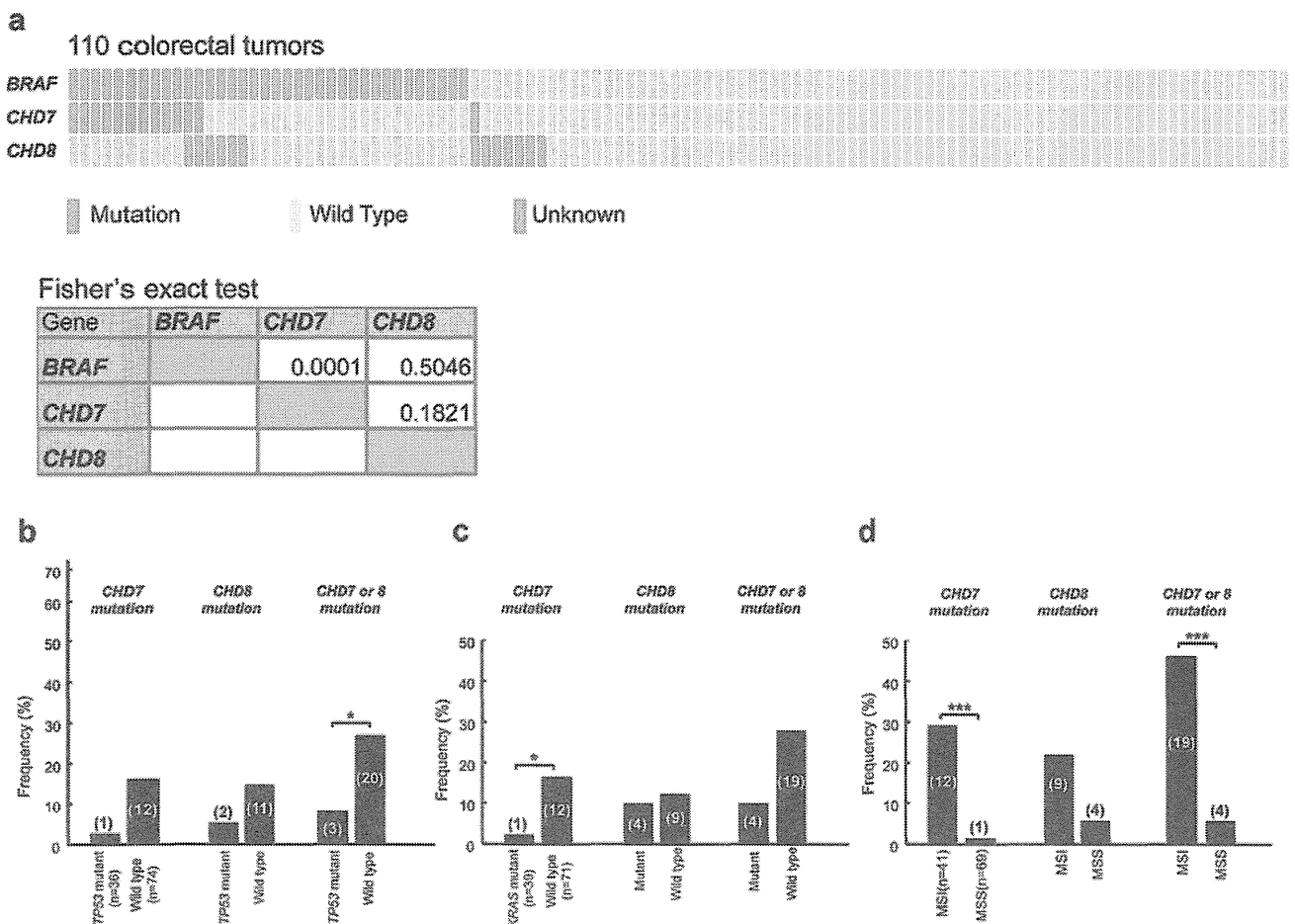
Supplementary Figure 1. Representative pyrograms (A and B) and sequencing chromatograms (C) for 3 of 4 randomly selected genes mutated in the discovery set.



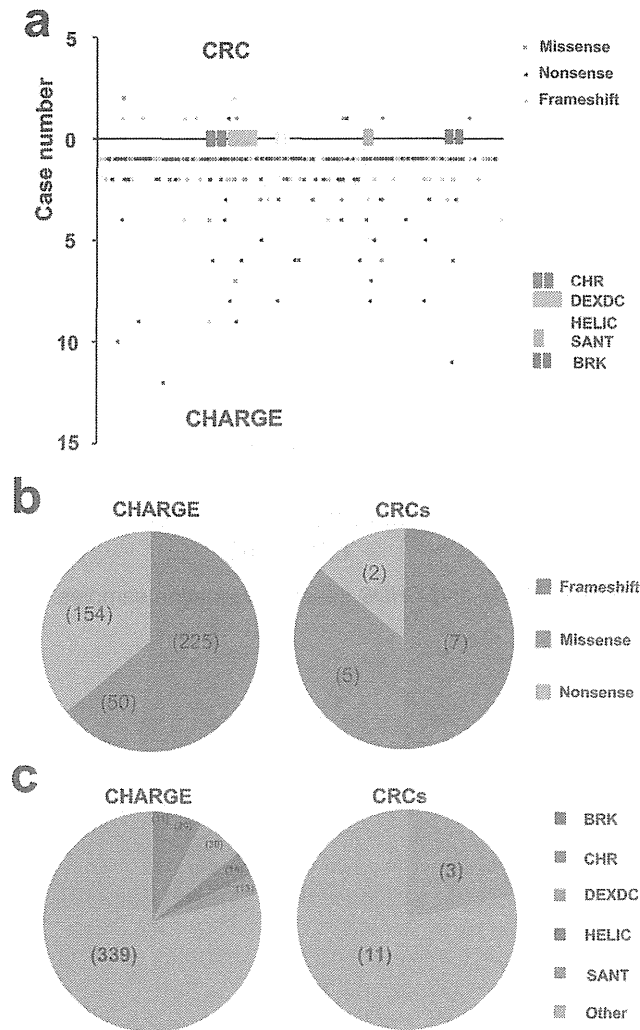
Supplementary Figure 2. Venn-diagram representing the number of genes mutated in CIMP1 CRCs, microsatellite stable/wild-type *BRAF* CRCs, and non-CIMP-high/unmethylated/wild-type *BRAF* CRCs in our study and 2 other studies. Nearly 3000 genes were mutated exclusively in the CIMP1 CRCs.



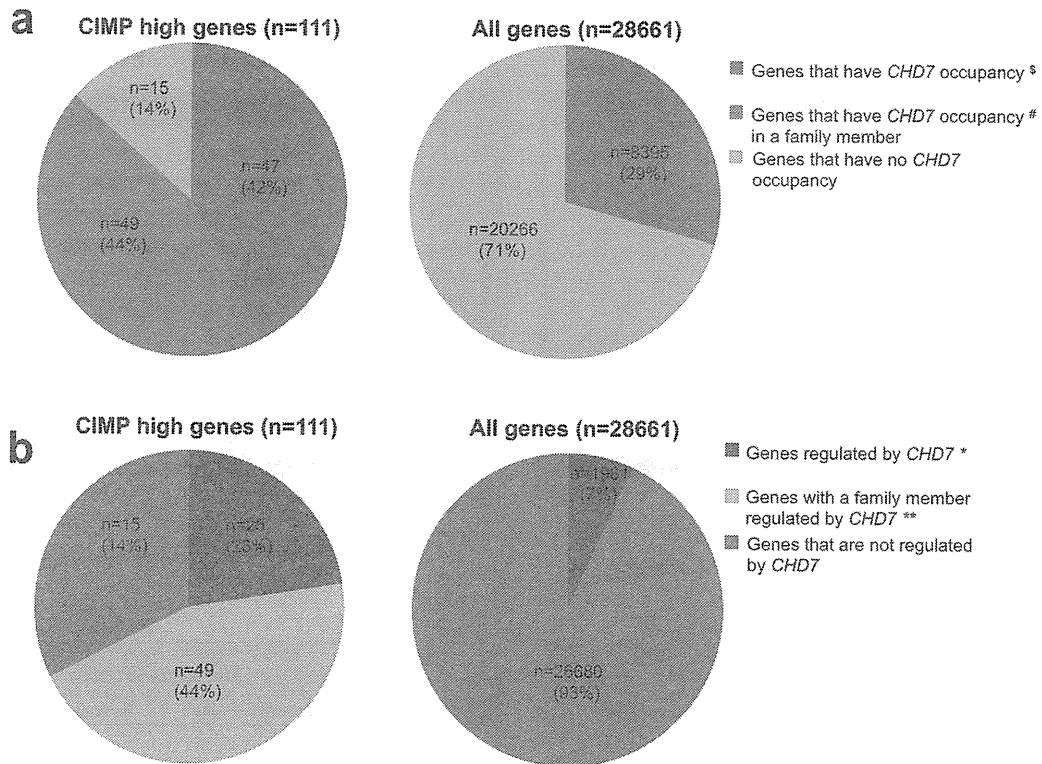
Supplementary Figure 3. Representative sequencing chromatograms of *CHD7* and *CHD8* genes in validation samples.



Supplementary Figure 4. Presence of mutations in *BRAF*, *CHD7*, and *CHD8* in 110 colorectal tumors (A). *P* values of Fisher's exact test are shown. *BRAF* and *CHD7* show a strong tendency of co-occurrence in the test samples. Prevalence of *CHD7* and *CHD8* mutations by different *TP53* (B) and *KRAS* mutations (C) and microsatellite stability status (D). Numbers in parentheses represent the number of mutated cases. MSI, microsatellite instability; MSS, microsatellite stability. **P* < .05; ****P* < .001.



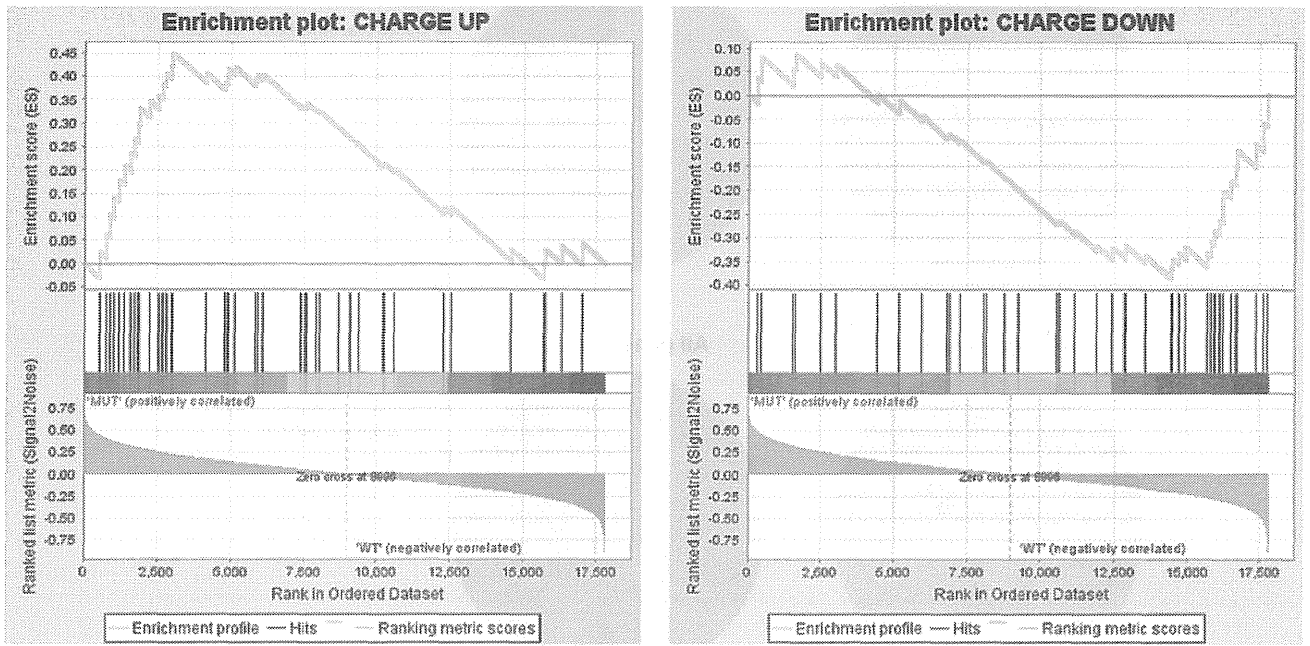
Supplementary Figure 5. Comparison of *CHD7* mutation spectra in CHARGE syndrome and CRC. A total of 429 nonsilent pathogenic coding sequence mutations in CHARGE syndrome (from the database www.chd7.org) were used for this analysis. (A) Overview of nonsilent pathogenic coding sequence mutations in CHARGE syndrome (*upper*) and CRC (*lower*). Each plot represents a single mutation, and the x-axis represents the number of reported cases. (B, C) *CHD7* change types (B) and distribution across domains (C) in CHARGE syndrome (*left*) and CRC (*right*). Numbers in parentheses represent number of mutations. BRK, BRK domain; CHR, chromatin organization modifier domain; DEXDC, DEAD-like helicase superfamily; HELIC, helicase superfamily C-terminal domain; SANT, “SWI3, ADA2, N-CoR and TFIIB” DNA-binding domains.



Supplementary Figure 6. Enrichment of *CHD7* occupancy in frequently methylated genes in CIMP-positive CRCs (A) and greater influence of *CHD7* gene knockdown on gene expression change (B). The genes used for comparisons were hypermethylated with a β -value difference >0.20 and showed >2 -fold decrease in their gene expression levels in CIMP-high tumors, as reported by Hinoue et al¹⁸ ($n = 111$). Genes bound by Chd7 in mouse neural stem cells (Engelen et al¹⁷) and altered expression after knockdown of *CHD7* in mouse ES cells (Schnetz et al¹⁹) were considered to be regulated by *CHD7*. §CIMP genes, $P = .003$; §,#CIMP genes and their family members, $P < .00001$ compared with all genes. *CIMP genes, $P < .00001$; *, **CIMP genes and their family members, $P < .00001$ compared with all genes.

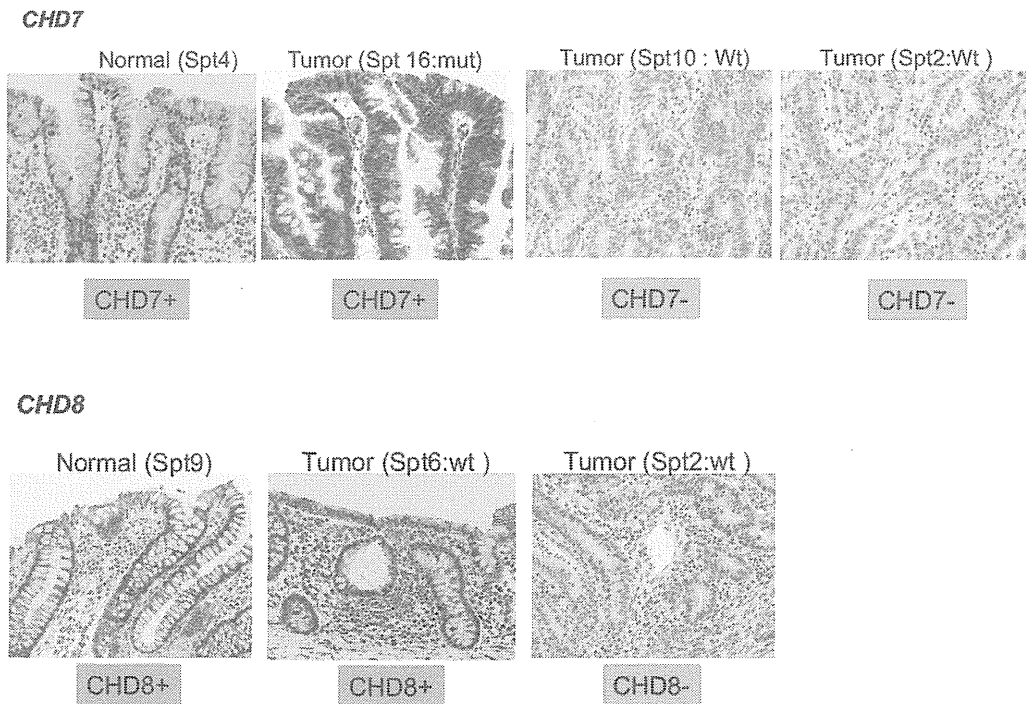
ES 0.45 FDR 0.04
 NES 1.53 FWER 0.03

ES -0.39 FDR 0.07
 NES -1.39 FWER 0.04



GSEA on TCGA CRC dataset (*CHD7*-mut versus *CHD7*-wt)

Supplementary Figure 7. Enrichment of genes up-regulated and down-regulated in CHARGE syndrome among classifiers of *CHD7*-mutant CRCs. GSEA, gene set enrichment analysis; MUT, mutant; WT, wild type.



Supplementary Figure 8. Immunohistochemical (IHC) analysis of *CHD7* and *CHD8* in normal colon and colorectal tumors with and without *CHD7/8* mutations.

